THERMAL NOISE IN INSULATOR DIODE WITH TRAPS LYING BELOW THE FERMI LEVEL UNDER CDDM REGIME

V. S. RAGHAV, Y. K. SHARMA AND C. S. AGARWAL
Department of Physics, R.B S. College, Agra 282 003, India.

ABSTRACT

The effects of space charge and traps on the thermal noise in one carrier insulator diode with traps lying below the Fermi level have been studied using the regional approximation method. The mobility of the current carriers is proportional to the carrier density. It is shown that the noise is highly suppressed by the space charge present in the device.

THE conductivity of single injection devices is modulated by injected charge carriers when current flows giving nonlinear current-voltage characteristic. It is possible to construct solid state devices from crystals of extremely pure germanium and silicon, where dc and ac properties are very close to the predicted theoretical models. Therefore, an attempt has been made to study theoretically the effects of space charge and traps on the noise in an insulator operating under carrier density-dependent mobility (CDDM) regime on the basis of the theory given earlier[1], which has been experimentally verified for the space-charge-limited solid state diodes without considering the trapping effect[2].

Single injection in an insulator involves current flow by electrons or holes. The injection is kept at levels such that the current flow is limited by space charge. The presence of traps drastically affects the current flow[3-5]. It also affects the noise generated in the device which is due to current or voltage fluctuations caused by the scattering of the current carriers at the lattice imperfections present in the insulating materials[6,7]

There is another source of noise in diodes associated with the injection process which is considered as a series of single events occurring randomly. The injection noise is known to play an important role in vacuum diodes[6]. Analogously, it was considered by several workers in the earlier studies of noise in soild state diodes[8,9], that the injection noise is the main source of noise in such devices. But, the experimental studies have proved that the injection noise is negligibly small in comparison to thermal noise which is due to the fact that the space charge reduces the injection noise[8 9] much lower than the thermal noise[7]. Thus the thermal noise is the main source of noise generated in the space-charge-limited solid state diodes.

REGIONAL APPROXIMATION METHOD

Consider a low mobility insulator containing significant density of a single set of traps lying below the Fermi level. Assuming the conduction through electrons, the general equations characterizing the current flow and Poisson's law are given by

$$J = e\mu n E, \quad n = n_0 + n_i, \tag{1}$$

$$\frac{\epsilon}{e}\,\frac{dE}{dx} = n_i - n_{ti} = (n + n_0) + (n_t - n_{t,0}), \tag{2}$$

$$= (n - n_0) + (p_{t,0} - p_t), \tag{3}$$

where

$P_t = N_t - n_t$ and $P_{t,0} = N_t - n_{t,0}$,

μ is the mobility of the current carriers, ϵ the permittivity of the insulator, n_i and $n_{t,i}$ are the injected free and trapped electron concentrations, n the concentration of free electrons and n_0 the thermally generated free electrons, n_t and $n_{t,0}$ are the trapped electrons and its thermal equilibrium value, p_t and $p_{t,0}$ are the concentrations of traps not occupied by electrons and its thermal equilibrium value corresponding to n and n_0 respectively, and N_t the total number of traps present in the insulator. The total current flow is the additive contribution of two components: (a) thermal free electrons n_0 and (b) injected electrons $n_i = n - n_0$. Thermal free carriers contribute to current but not to space charge.

In low mobility insulators[10], some trapping sites may be permanently occupied so that they do not contribute any delay by trapping the moving carriers. This gives rise the mobility of the current carriers as a function of carrier density

$$\mu = hn(x), \tag{3}$$

where h is the proportionality constant. The equations are subjected to a boundary condition usually employed in single injection current theories for Ohmic contact

$$E(0) = 0. \tag{4}$$

At low injection level of current, the insulator is divided into three separate regions using the regional approximation method[3-5,12]. The injected current carriers n_i decreases monotonically from a higher value at cathode. All the injected carriers forming the space charge are not reached to anode at appropriate injection level of current. There will be an imaginary transition plane $x_2(J)$ where $n_i(x_2)=n_0$. To the right of plane x_2, $n_0>n_i$, and n_i may be neglected; to the left of plane, $n_i>n_0$, and n_0 is neglected. Due to the presence of additional term $(p_{t,0}-p_t)$ in Poisson's law (2), the space charge region $(0\leq x\leq x_2)$ may further be divided into two separate regions. For $n_i=n_0$, $n=n_0+n_i=2n_0$ which corresponds to $p_t=p_{t,0}/2$. Therefore, $p_t<p_{t,0}/2$ in the left of the plane x_2 and p_t is neglected in equation (2). Now, there will be a transition plane x_1 where $=n_i(x_1)=n(x_1)=p_{t,0}$. To the left of plane x_1, $n>p_{t,0}$ and $p_{t,0}$ is neglected; and to the right of plane x_1, extending upto x_2, $P_{t,0}\simeq(p_{t,0}-p_t)>(n-n_0)$ so that $(n-n_0)$ as well as p_t are neglected in (2). The sets of defining equations for current flow and Poisson's law in three regions are summarized in figure 1.

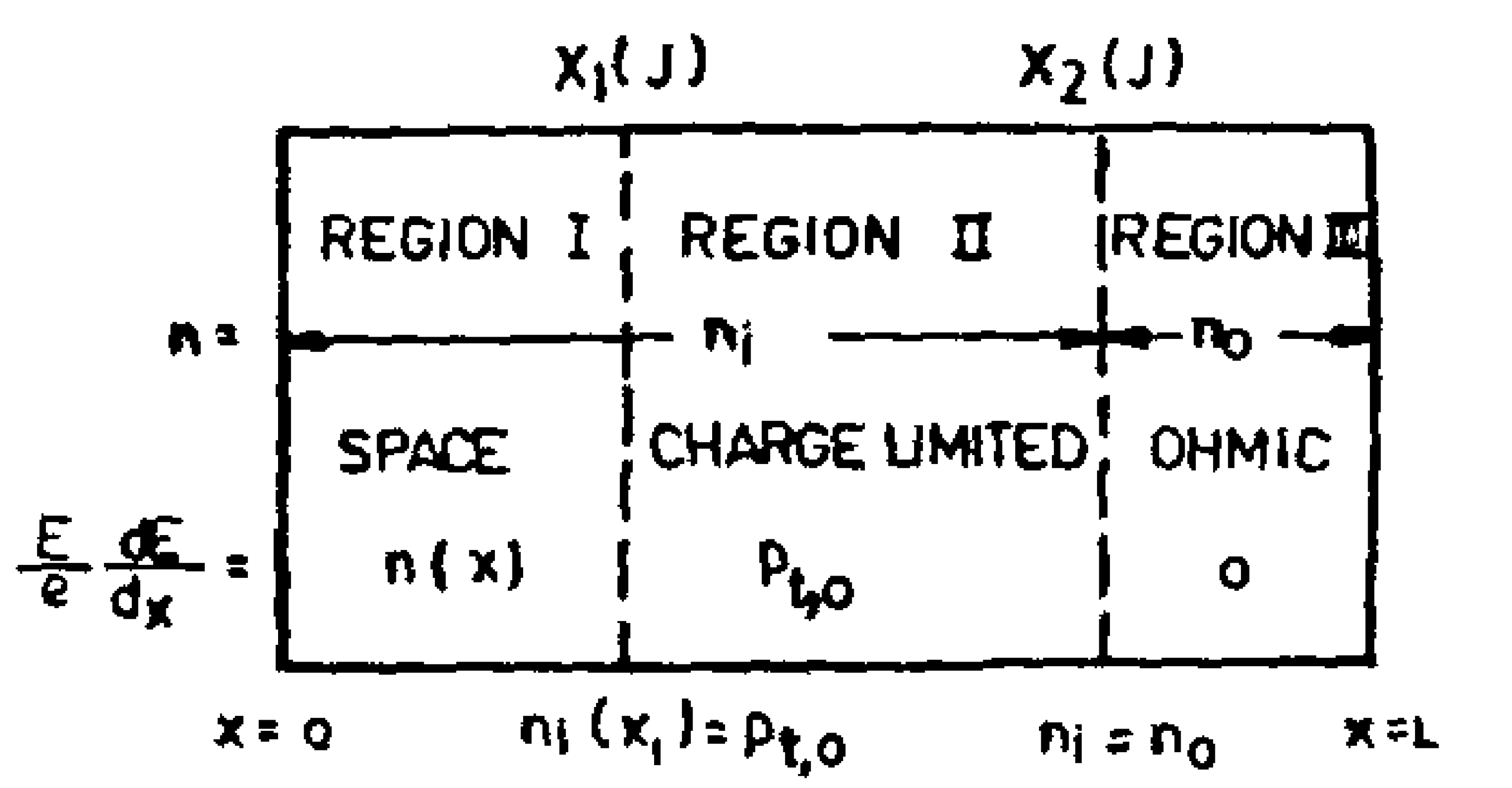

Figure 1. Schematic regional scheme for the current injection in a low mobility insulator with traps lying below the Fermi level. The dotted vertical lines represent the imaginary transition planes.

As shown in figure 1, three regions are well separated by two imaginary transition planes x_1 and x_2 which are shifting towards anode with increasing current. Regions I and II are space-charged-limited and the region III is ohmic. The distances x_1 and x_2 are given by[12]

$$x_1=\frac{2\epsilon J}{3e^2hA^3n_0^3},\quad x_2=\frac{\epsilon J}{e^2hn_0^3A}. \tag{5}$$

where $A=P_{t,0}/n_0$.

It is evident from (5) that the planes x_1 and x_2 are the function of current density. These transition planes represent the hallmark for the different current-voltage regimes in the complete current-voltage characteristic as described below

$$x_1(J_{cr,2})=L,\quad x_2(J_{cr,1})=L,$$

where $J_{cr,1}$ and $J_{cr,2}$ are the critical currents corresponding to the injection levels at which the region III and II respectively leave the insulator.

THERMAL NOISE IN THE DIODE

The interaction of the current carriers with the lattice of insulator results in current or voltage fluctuations which generates the noise in the diode. A very simple method of noise calculation in space-charge-limited single injection solid state diode has been given earlier[1,7]. The sample is subdivided conceptually into small slabs by the planes perpendicular to the current flow. The sum of voltage drops across each slab gives the total voltage fluctuation in the open circuited device.

The open circuited noise emf in a frequency interval Δf is represented[7] by $\overline{\Delta v^2}$, where

$$\overline{\Delta v^2}=4kT\Delta R\Delta f,\quad \Delta R=\frac{\Delta x}{e\mu nS}=\frac{E\Delta x}{JS}, \tag{6}$$

here ΔR is the resistance of the small section Δx and S the area of cross-section of the diode. Summing over all sections of the diode, equation (6) becomes

$$\overline{v^2}=4kTR\Delta f,\quad R=\Sigma\Delta R=\frac{V}{JS}, \tag{7}$$

where the voltage developed across the diode length L is given by

$$V=\int_0^L E(x)\,dx. \tag{8}$$

The noise generated in all the three regions of the insulator is estimated in the complete range of current-voltage characteristic in terms of mean square noise voltage as follows:

(i) True Ohm's regime ($J\ll J_{cr,1}$), $x_2\ll L$. In this regime, the injection level is such that the regions I and II are negligibly small and the contribution is mainly given by region III. Injected free and trapped carriers are negligibly small in region III, therefore all the terms in the left hand side of Poisson's law (2) are neglected. Then, (1) to (4) give the current-voltage characteristic

$$J=ehn_0^2\frac{V}{L}, \tag{9}$$

which is pure Ohm's law ($J\propto V$). The Ohmic resistance and noise is evaluated from (7) and (9)

$$R_\Omega=\frac{L}{ehn_0^2S},\quad \overline{v_\Omega^2}=4kTR_\Omega\Delta f, \tag{10}$$

which is a constant value.

(ii) Ohmic regime ($J<J_{cr,1}$), $x_2<L$. The regions II and III are dominant inside the insulator. The total voltage developed across the diode (derived from

current equation, Poisson's law and (8) for regions II and III) is the sum of the voltages across the regions II and III,

$$V = V_{II} + V_{III} = \frac{e n_0 A x_2^2}{2\epsilon} - \frac{J x_2}{3 e h A^2 n_0^2} + \frac{J(L - x_2)}{e h n_0^2}, \qquad (11)$$

where x_2 is given in (5). Equations (7) and (11) are used to give the noise,

$$R_0 = \frac{V}{JS} = \frac{(V_{II} + V_{III})}{JS}, \ \overline{v_0^2} = 4kTR_0\Delta f. \qquad (12)$$

At the critical current $J_{cr,1}$, $x_2 = L$, then (11) and (12) give

$$R_{cr,1} = \frac{V_{cr,1}}{J_{cr,1} S} \approx \frac{L}{2 e h n_0^2 S}, \ v_{cr,1}^2 = 4kTR_{cr,1}\Delta f. \qquad (13)$$

(iii) TFL regime ($J_{cr,1} < J < J_{cr,2}$), $x_1 < L < x_2$. The space charge regions I and II are present in the insulator. The noise generated in the device is obtained as

$$R_{TFL} = \frac{V}{JS} = \frac{V_I + V_{II}}{JS}, \ \overline{v_{TFL}^2} = 4kTR_{TFL}\Delta f, \qquad (14)$$

where the voltages V_I and V_{II} are given by

$$V_I = \frac{3}{5}\left[\frac{9eJ}{4\epsilon^2 h}\right]^{1/3} x_1^{5/3}, \qquad (15)$$

$$V_{II} = \frac{e n_0 A}{2\epsilon}(L^2 - x_1^2) - \frac{J(L - x_1)}{3 e h A^2 n_0^2},$$

which are derived from various sets of equations given elsewhere[12] The terminating noise for trap-filled-limit (TFL) regime is obtained from (14) and (15) with $x_1 = L$,

$$R_{cr,2} = \frac{V_{cr,2}}{J_{cr,2} S} = \frac{3L}{5A^2 e h n_0^2 S},$$

$$\overline{v_{cr,2}^2} = 4kTR_{cr,2}\Delta f. \qquad (16)$$

(iv) Trap-free regime ($J > J_{cr,2}$), $x_1 > L$. The region I entirely fills the insulator. All the traps are filled with electrons and the insulator works in pure space charge conditions. Terms other than n in (2) may be neglected. Then, (1)–(4) give the current-voltage characteristic for SCL trap free regime as

$$J = 2.06 \frac{\epsilon^2 h}{e} \frac{V^3}{L^5}. \qquad (17)$$

which yields the noise generated in trap free regime as

$$R_s = \frac{V}{JS} \approx \frac{eL^5}{2hS\epsilon^2 V^2}, \ \overline{v_s^2} = 4kTR_s\Delta f, \qquad (18)$$

which shows that the mean square noise voltage decreases as the inverse of square of the applied voltage in space-charge-limited trap free regime.

Discussion

The noise factor $[\overline{v^2}/kT\Delta f]$ versus applied voltage is plotted on a log-log scale in figure 2 by using (10)–(18). The noise is large in the Ohmic regimes (i)

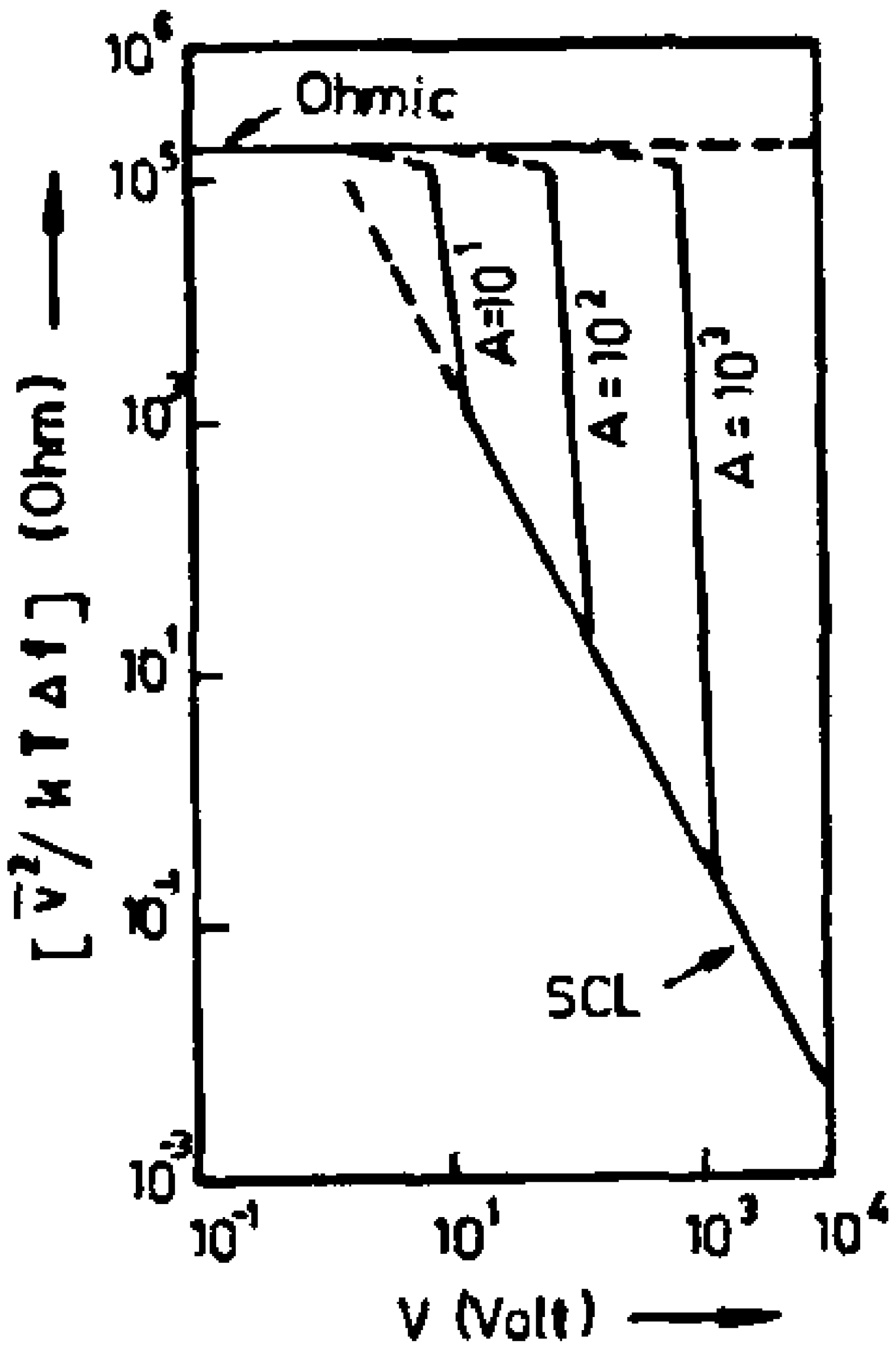

Figure 2. Log-log plot of the noise factor $(\overline{v^2}/kT\Delta f)$ versus applied voltage for three values of parameter $A = 10^1$, 10^2 and 10^3.

and (ii) of the insulator and very much reduced in the space-charge-limited regimes (iii) and (iv) described in section 3. The noise factor decreases with the increase of voltage from a very high value in true Ohm's regime to the lower values in the SCL trap-free regime by several decades. The vertical decrease in noise is during the trap-filled-limit (TFL) regime where the traps are gradually filled with electrons. It is due to this that the effect of traps on thermal noise is observed in TFL regime. It might be possible that in TFL regime the trapping noise is highly increased whose study may be made on the basis of previous work[11]. Thus, the noise is highly suppressed by the space charge present in the device.

1. Van der Ziel, A., *Solid State Electron*, 1966, **9**, 899.
2. Hsu, S. T., Van der Ziel, A. and Chenette, E. R., *Solid State Electron*, 1967, **10**, 129.
3. Sharma, Y. K., *Phys. Rev.*, 1974, **B10**, 3273.
4. Sharma, Y. K., *J. Appl. Phys.*, 1982, **53**, 1241.
5. Lampert, M. A. and Mark, P., *Current injection in soilds*, Academic Press, New York, 1970.

6. Van der Ziel, A., *Noise*, Prentice Hall, Englewood Cliffs, New Jersy, 1954.
7. Van der Ziel, A., *Proc. IEEE*, 1970, **58**, 1178.
8. Van der Ziel, A., *Solid State Electron*, 1966, **9**, 123.
9. Sergiescu, V., *Br. J. Appl. Phys.*, 1965, **16**, 1435.
10. Wintle, H. J., *J. Appl. Phys.*, 1972, **43**, 2927.
11. Zijlstra, R. J. J. and Driedonks, F., *Physica*, 1970, **50**, 331.
12. Sharma, Y. K., *Indian J. Pure Appl. Phys.*, 1980, **18**, 812.

DNA-POLYCATION INTERACTIONS:UREA DEPENDANCE

V. H. MULIMANI, M. MADAIAH AND R. A. DAY†

Department of Chemistry, Karnataka University, Dharwad 580 003, India.

† Department of Chemistry, University of Cincinnati, Cincinnati, Ohio 45221, USA

Abstract

Thermal denaturation of DNA in the presence of novel polycations has been studied at varying concentrations of sodium chloride and urea. T_m values of DNA-polycation complexes decreased linearly with increasing urea concentrations. It is proposed that urea is responsible for destroying intermolecular hydrogen bonds and hydrophobic interactions which may be involved in the maintenance of tertiary structure of DNA-polycation complex. Both electrostatic and hydrophobic effects probably influence the stability of the DNA-polycation complex.

Introduction

It is well known that various types of polycations interact strongly with nucleic acids which are polyanions[1-10]. The effects of urea on the secondary structure of nucleic acids have been extensively investigated[11,12]. The effects of high concentration of urea on the macromolecular structure and interaction are well known. These arise from competitive hydrogen bonding and disruption of hydrophobic interactions[13]. Such effects frequently show co-operativity and do not arise below critical concentrations. However with small molecules whose residues may be incorporated into macromolecules, the effects may be detected at low concentrations of urea or urea derivatives and follow linear or monophasic functions to higher concentrations[14]. Thermal denaturation studies have been utilised to probe the interactions of basic proteins and other polycations with DNA[15]. In this paper we report our investigations on the melting behaviour of polycation-DNA complex in different concentrations of urea.

Methods and Materials

DNA was purchased from Sigma Chemical Company (USA) as its sodium salt (sodium deoxynucleotide of calf thymus DNA highly polymerised). Sodium deoxynucleate (1 mg/ml) was added to SSC buffer (sodium chloride 0.01 M and sodium citrate 0.001 M pH 7) over a few drops of carbon tetrachloride. The exact amount of DNA was estimated spectrophotometrically assuming $\epsilon = 6.6 \times 10^3\ cm^{-1} M^{-1}$ at 260 nm. The A_{260}/A_{230} ratio of this solution was 2.3. The following polycations were synthesised according to the procedure of Rembaum and coworkers[16,17].

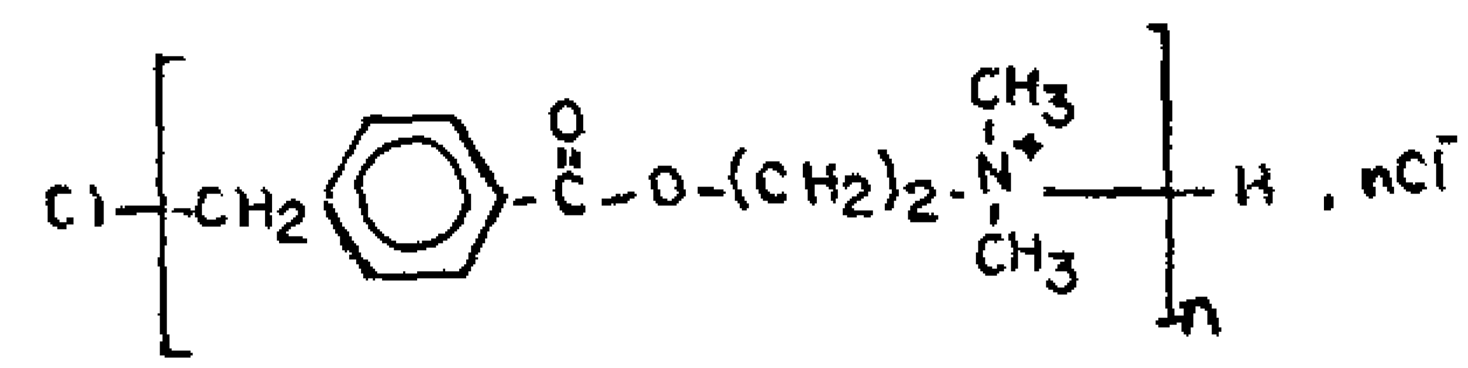

POLYCATION I $n = 35 \pm 5$

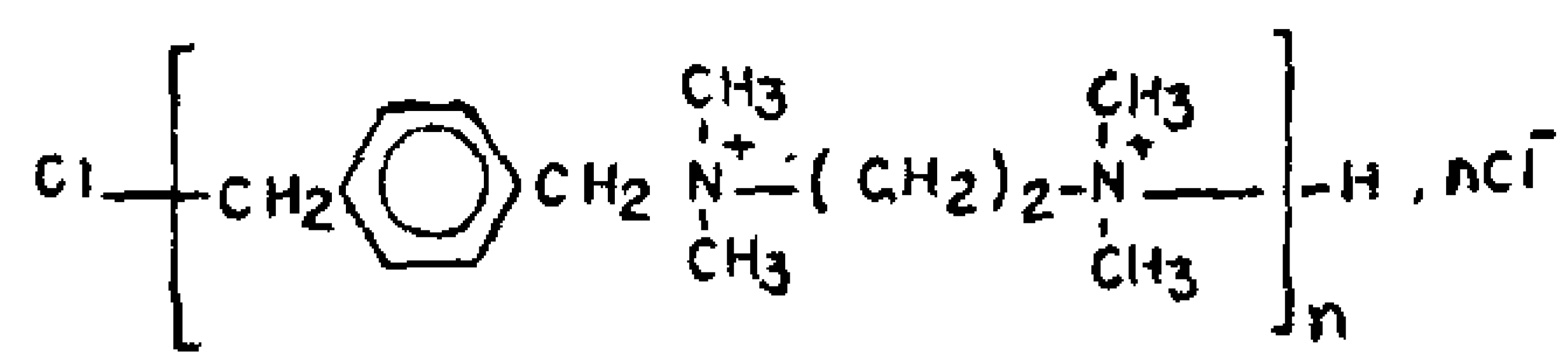

POLYCATION II $n = 10$

Stock solutions were prepared in the following concentrations: DNA (1 mg/ml) in sodium chloride 0.01 M and sodium citrate 0.001 M pH 7, polycation (0.01 M), sodium chloride (1 M) and urea (10 M). The reaction mixture contained the following order: DNA(7.5×10^{-5} in DNA phosphate), sodium chloride, EDTA (0.001 M), polycation and urea. The total volume of the mixture was made up to 4 ml by diluting with an appropriate volume of SSC buffer. The polycation and DNA ratio is represented by r. Before determining melting temperature (T_m) the UV absorbance of the